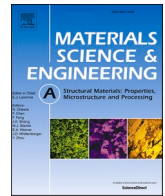




Contents lists available at ScienceDirect

Materials Science & Engineering A

journal homepage: <http://www.elsevier.com/locate/msea>

The damage mechanism of 17vol.%SiC_p/Al composite under uniaxial tensile stress

Qiuyan Shen^{a,b}, Zhanwei Yuan^{a,b,*}, Huan Liu^{a,b}, Xuemin Zhang^a, Qinqin Fu^c,
Quanzhao Wang^{d,**}

^a School of Materials Science and Engineering, Chang'an University, Xi'an, Shaanxi, 710061, China

^b Laboratory of Advanced Technology and Equipment, Chang'an University, Xi'an, Shaanxi, 710061, China

^c Center for Advancing Materials Performance from the Nanoscale (CAMP-Nano), Hysitron Applied Research Center in China (HARCC), State Key Laboratory for Mechanical Behavior of Materials, Xi'an Jiaotong University, Xi'an, Shaanxi, 710049, China

^d Institute of Metal Research, Chinese Academy of Sciences, Shenyang, 110016, China

ARTICLE INFO

Keywords:

SiC_p/Al composite
Damage behavior
Fracture mechanism
Finite element method
Stress-state

ABSTRACT

In this paper, the deformation, fracture and damage behavior of SiC_p/Al composites are studied by experiments and finite element analysis. The crack cracking process of the material was observed by in-situ tensile test, it was found that the composite first produced microcracks near the particles, and the cracks mainly spread to depth and then to both sides. It is determined by a tensile test that the fracture mechanism of the material is the tearing of the aluminum matrix and the peeling between the particles and the matrix. The tensile damage mechanism of the composite material in three directions (rolling direction, rolling transverse direction and rolling normal direction) and different strains were determined. It is found that in the process of tensile deformation, microcracks are first formed at the defects (voids) and weak interfaces, and many fine cracks converge together to form large cracks leading to the fracture of the material, during which a few particles fall off, but there is no particle fracture. The global and local tensile tests of the composites were simulated by finite element method, the results of the stress-strain state under different strains and the effects of particles on the materials are analyzed in detail, and the validity of the test results is determined.

1. Introduction

With high stiffness and strength, fatigue resistance, wear resistance, creep resistance and excellent thermoelectric properties, particle reinforced metal matrix composites (PRMMCs) are widely used in high-tech fields such as aerospace, advanced weapon systems, and the automotive industry [1–5]. Among many types of PRMMC, silicon carbide particle reinforced aluminum matrix composites (SiC_p/Al) are widely used in automotive brake discs, electronic components and bearing components because of their high specific strength and specific modulus, fatigue resistance and high dimensional stability [4–7]. Among them, SiC_p/Al composites with low volume fraction (generally no more than 20 vol%) are mainly used in structural materials, which will cause damage in the process of deformation and load, thus reducing the serviceability. In order to ensure the high precision and high requirements of the material, it is very important to understand the deformation, damage and fracture

behavior of this type of composites.

The damage of SiC_p/Al composites includes the damage of different components, matrix, SiC particles and interface. For example, the damage of the matrix is mainly manifested by the void nucleation and growth of the matrix material in the process of deformation [8–10]. The characteristics of particles also have an effect on the deformation damage of the composites, such as the size, shape and distribution of particles, which is mainly the brittle fracture of particles [11–13]. Williams et al. [8] studied the damage behavior of SiC_p/2080Al composites by X-ray synchrotron tomography, and found that the damage area of the composites was limited to a very small volume near the fracture surface, and the particles with larger size and larger aspect ratio were more likely to fracture. They also established three-dimensional finite element models of the sphere and ellipsoid based on the real microstructure, and found that particles with sharp corners have a large load transfer effect [14]. Zhang et al. [15] studied the damage mechanism of

* Corresponding author. School of Materials Science and Engineering, Chang'an University, Xi'an, Shaanxi, 710061, China.

** Corresponding author.

E-mail addresses: yuanyekingfly@163.com (Z. Yuan), qzhwang@imr.ac.cn (Q. Wang).

<https://doi.org/10.1016/j.msea.2020.139274>

Received 17 February 2020; Received in revised form 16 March 2020; Accepted 18 March 2020

Available online 23 March 2020

0921-5093/© 2020 Elsevier B.V. All rights reserved.

Table 1
Chemical composition of 2009 aluminum alloy.

Element	Cu	Mg	Si	Fe	Al
Wt. %	3.8%	1.4%	0.14%	0.1%	Bal.

particle reinforced metal matrix composites by establishing finite element models. Sozhamannan et al. [16] simulated the uniaxial tensile test of SiC/Al composites by finite element method, and found that particle fracture, interfacial debonding, volume fraction and size of particles were the main causes of PRMMC failure. Jie et al. [17] studied the tensile fracture behavior of SiC_p/Al composites and found that stress concentration leads to particle fracture and interface peeling, which reduces the bearing capacity of the composites and accelerates the damage accumulation process. Up to now, although there are many studies on the effects of particle shape, size and volume on the damage of composite [18–21], the microscopic evolution in the deformation process is rarely introduced, so it is impossible to analyze the internal mechanism of material damage. Therefore, it is necessary to have a detailed understanding of the deformation state and microstructure changes of the composites during the loading process.

In this study, in-situ tensile and loading-unloading tensile tests were used to study the damage and failure of SiC_p/Al composites in three directions (rolling direction, rolling transverse direction and rolling normal direction) and four different deform degree. The finite element model based on 3D element reproduces the evolution of stress and strain in the deformation process of composites, to reveal the internal failure mechanism of composites during the process of tensile fracture.

2. Experiment

The material used in this study (17vol%SiC_p/2009Al) was first made by powder metallurgy and then made into plates by extrusion and rolling techniques. In this composite, the particle size distributed within the range of 1–15 μm, and the major size is 4–8 μm. The thickness of the plate is 2 mm and the standard composition of 2009Al is listed in

Table 1. Considering the impact of rolling technology on the material, three directions of the sample were selected for research. The microstructure of SiC_p/Al composites is shown in Fig. 1, in which SiC particles are relatively fine and polygonal, the dispersion of single particles is poor, and the particles are agglomerated. It can be seen from Fig. 1(c) that the distribution of SiC particles in the rolling normal is about half of the other directions, but the particle size is about twice that of the other directions. The standard uniaxial tensile samples with cross-section of 5 mm × 2 mm and standard distance of 30 mm and the in-situ tensile samples with cross-section of 3 mm × 1.8 mm and standard distance of 33 mm are prepared along the rolling direction of the plate. A notch of about 1 mm in length and width was preset at the center of the side of the in-situ tensile specimen. Before the material is tested, all samples were annealed at 350°C for 2 h in a heat treatment furnace to eliminate the effect of internal stress on subsequent tests.

The average elongation δ of the material is determined by tensile test on the MTS CMT5105 testing equipment, and the tensile rates are 0.1 mm/min, 0.5 mm/min, 1 mm/min and 2 mm/min, respectively. Then the uniaxial tensile loading and unloading tests were carried out, and the strains of the composites were 0.2δ, 0.4δ, 0.6δ and 0.8δ respectively during unloading, the microstructure of the obtained fracture surface was observed by SEM. After loading and unloading, the specimen with large deformation in the middle was taken for microstructure observation. The hardness values of different positions of the damaged samples were measured by Vickers hardness tester.

3. Results and discussion

3.1. In-situ tensile test

By dynamically observing specimen during the in-situ tensile test, it is used to understand the process of crack initiation and propagation of SiC_p/Al composites. The stress-strain curve and crack propagation mode recorded during in-situ tension of SiC_p/Al composites is shown in Fig. 2. The in-situ tensile specimen is parallel to the rolling direction. Fig. 2(e) is a schematic diagram of the structure of the material in three

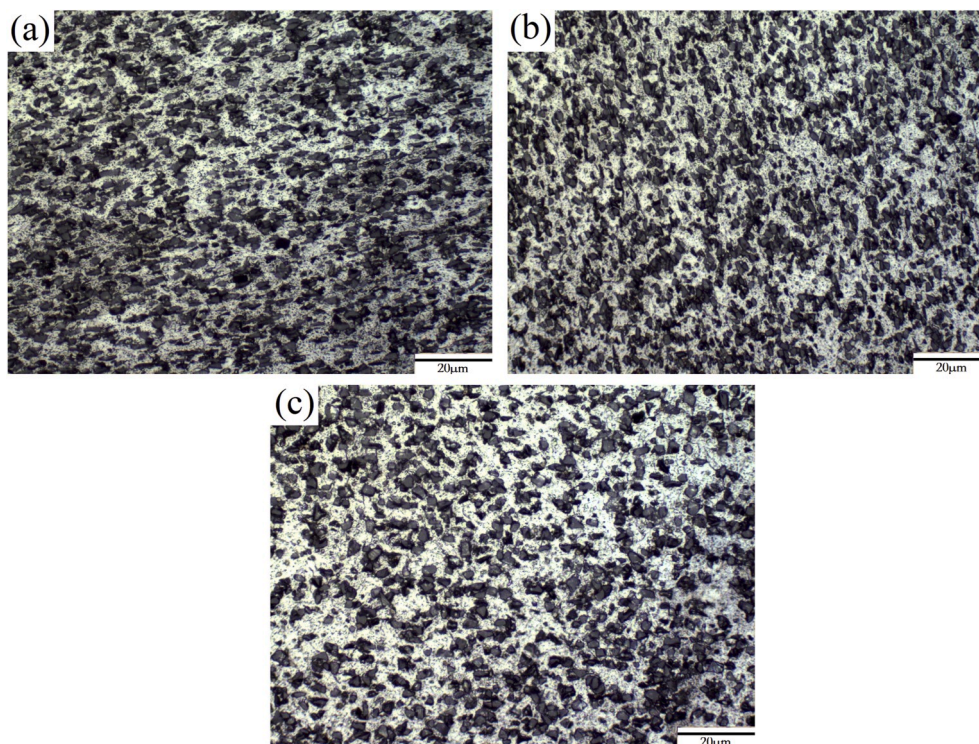


Fig. 1. Microstructures of SiC_p/Al composites in three directions: (a) rolling direction, (b) rolling transverse direction, (c) rolling normal direction.

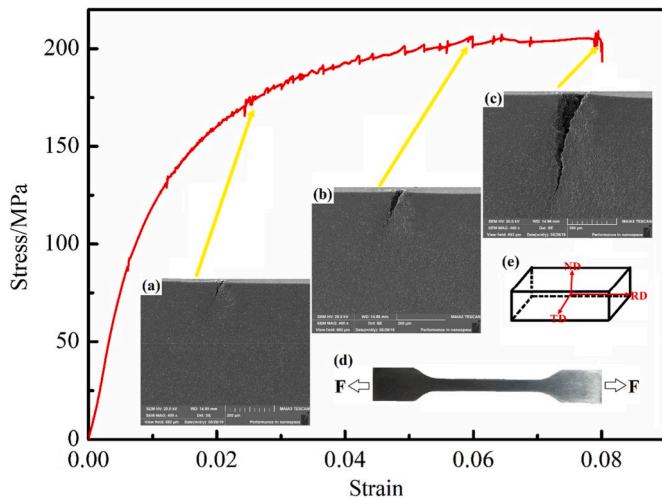


Fig. 2. Stress-strain curve of in-situ tensile test and image of the crack under different displacements during in-situ SEM. (a): 0.742 mm, (b): 1.976 mm, (c): 2.641 mm, (d): In-situ tensile specimen diagram, (e): Schematic diagram of the structure in three directions.

directions. For convenience, TD, RD and ND in this paper represent rolling transverse direction, rolling direction and rolling normal direction, respectively. It can be seen from the curve that in the elastic deformation stage, the stress increases sharply with the increase of

strain. After entering the stage of plastic deformation, the curve appears sawtooth shape, which is mainly related to dynamic strain aging and the dynamic interaction between solute atoms and movable dislocations. It can be seen from the figure that the crack mainly spreads on the vertical surface of ND, and the early crack propagation direction is about 60° with the loading direction, and then propagates to the vertical direction. As shown in Fig. 2(a), when the stress is 175 MPa, the crack length is $100\ \mu\text{m}$ and the width is $15\ \mu\text{m}$. At the same time, it is found that the crack propagates gradually in the vertical plane of TD with the increase of stress. When the stress is 200 MPa, the depth of the crack increases by $5\ \mu\text{m}$ compared with the previous stage, but the width increases sharply by $25\ \mu\text{m}$ (Fig. 2(b)), shows that the crack propagates mainly along the vertical plane of TD at this stage. Subsequently, the crack propagates rapidly to the depth until the fracture (Fig. 2(c)).

The process of crack initiation and propagation is shown in Fig. 3. At the initial stage of loading, some microcracks are produced at the voids on the surface of the sample and at the weak interface between the particles and the matrix, and these microcracks gradually aggregation together (Fig. 3(b)). When entering the plastic deformation stage, a macroscopic crack approximately 60° to the tensile direction appears in Fig. 3(c) with the increase of deformation tension. Subsequently, the nearby microcracks began to grow, connect, and gradually converge with the macroscopic cracks, resulting in the shedding of a small amount of SiC particles (Fig. 3(c)). As the tension deformation continues to increase, while the crack continues to expand to the depth direction, it also begins to expand to the side (Fig. 3(d)). Although the propagation rate to the depth direction is very slow, the original crack gradually begins to

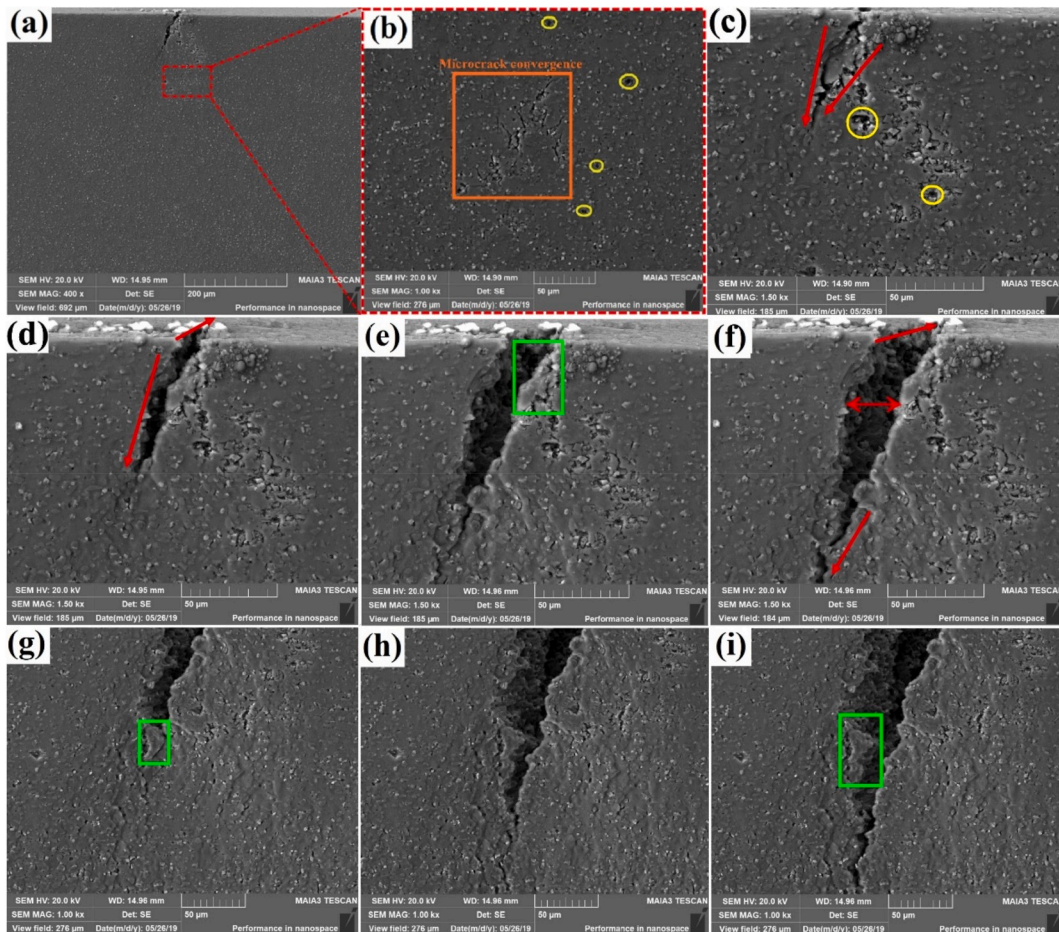


Fig. 3. Crack initiation and propagation process of SiC_p/Al composite. The orange and green boxes indicate the aggregation of microcracks and the poor bonding of the interface, respectively. Yellow circles indicate holes and particles fall off, and red arrows indicate the direction of crack propagation. (For interpretation of the references to colour in this figure legend, the reader is referred to the Web version of this article.)

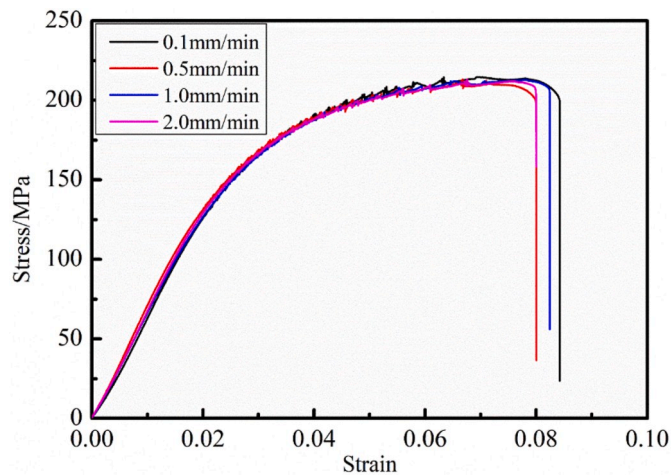


Fig. 4. Stress-strain curve of SiC_p/Al composite under uniaxial tension.

Table 2
Mechanical properties of SiC_p/Al composites.

Stretching rate	YS/MPa	UTS/MPa	Elongation/%
0.1 mm/min	141.1	214.4	8.4
0.5 mm/min	136.1	212.4	8.0
1 mm/min	137.3	212.8	8.2
2 mm/min	139.1	211.2	8.0

widen (Fig. 3(f)). When the tensile tension approaches the limit load, the crack propagates rapidly to the depth and gradually extends to the whole composite (Fig. 3(i)), resulting in the sudden fracture of the specimen. From the green box marks in the picture (Fig. 3(e), (g) and (i)), it can be seen that the SiC particles in the composites will affect the follow-up propagation path of cracks, especially in the areas of large particles and particle aggregation, where the interface is not well bonded. The crack extends along the particle boundary, which leads to the debonding or even shedding of SiC particles under the large stress field at the crack tip. In short, the damage process of SiC_p/Al composites includes crack initiation, crack propagation, crack connection, accompanied by the shedding of SiC particles.

3.2. Uniaxial tensile test

In order to study the damage evolution of SiC_p/Al composites during deformation in detail, the related tensile tests and loading and unloading tests were carried out. Different tensile rates were used in the experiment, and the effect of loading rate on the mechanical properties of the composites was analyzed. The stress-strain curves of the composites at different tensile rates are shown in Fig. 4. It can be seen from the tensile fracture result curves that the deformation curves under four different tensile rates have experienced a process from elastic deformation to plastic deformation and then to macroscopic fracture. In order to explore the effect of tensile rate on the tensile results, the yield strength (YS), ultimate tensile strength (UTS) and elongation obtained from the tensile stress-strain curve were statistically calculated (as shown in Table 2). It can be found from the data in the table that the three parameters of the tensile rate of 0.1 mm/min are slightly larger, but have no substantial effect. For SiC_p/2009Al composites, the average values of YS, UTS and elongation are ~ 138.4 MPa and ~ 0.081, respectively.

For particle reinforced aluminum matrix composites, the fracture mode of the material depends on the strength of the reinforced particles, the strength of the matrix and the interfacial bonding strength between the reinforced particles and the matrix [22]. When the interface bonding strength is small, it is easy to debond at the interface or a hole is formed at the sharp corner of the particles [17]. When the interface bonding

strength is greater than the matrix, the composite material will fracture along the matrix. Similarly, when the strength of the reinforced particles is less than the bonding interface, the particle fracture will occur. Fig. 5 depicts the typical fracture surface of SiC_p/Al composite at different tensile rates. It can be seen from the figure that there are many and deep dimples in the fracture surface of the composite, most of the dimples are very small. Some larger dimples with micron size can be seen, and there are a few SiC particles at the bottom (Fig. 5(f), and (h)). There are two reasons for the formation of dimples of the composite, namely, the interfacial debonding between the particles and the matrix or the ductile fracture of the matrix between the particles. For the shedding of particles, it is caused by the disharmony between particles and matrix deformation. When the crack initiation and propagation meets particles, many dislocations will accumulate at the interface and produce stress concentration. With the increase of strain, small cracks grow and merge together to form large cracks. When the interface between the reinforcement and the matrix is not strong, the crack will change its original direction and propagate along the weak-bond interface, and the particles will separate at the interface. Larger dimples are mostly caused by the agglomeration of SiC particles (agglomeration of SiC particles can be seen in Fig. 1). In general, cracks give priority to nucleation in the local area where agglomeration occurs. When the interface of the agglomeration region is closely bonded, the regional strain between the matrix and particles is relatively small. The agglomerated particles can deflect the crack and thus debond with the matrix, while numerous particles debonding can improve the tensile strength of the material. The matrix crack is seen in Fig. 5(a) and (b), which is the ductile fracture of the matrix caused by the plastic deformation. In addition, there are tearing edges and some microcracks (see Fig. 5(d) and (f)). Due to the addition of SiC particles, the fracture mode of the composite is different from that of aluminum and aluminum alloy, showing the characteristics of ductile-brittle fracture. The fracture mechanism of the composite is mainly caused by the tearing of aluminum matrix and the debonding of particles.

3.3. Microstructure observation and hardness

According to the results of tensile tests of SiC_p/Al composites, the average elongation δ of the composite is taken as 0.08. In order to explore the micro-damage evolution of the composites during deformation, the deformation degree 0.2 δ , 0.4 δ , 0.6 δ and 0.8 δ were selected as the unloading conditions of uniaxial tension. Fig. 6 shows the SEM of the composite under different strain conditions. It can be seen from Fig. 6(a), (d), (g) and (j) that in the RD, the defects-voids and shedding particles of the composites increase gradually with the increase of strain, and with the large size SiC particles fall off. The holes in the matrix gradually tear into large cracks with the increase of internal stress in the matrix, and the fracture of particles caused by tension is not observed. Fig. 6(b), (e), (h) and (k) shows the microstructure morphology of different strain in the TD, it can be seen that the change of TD is small with the increase of strain, in this direction, there is a small amount of SiC particles falling off, and some holes gradually appear around the particles. There is no large crack in the matrix. For the ND, it can be seen from Fig. 6(c), (f), (i) and (l) that there are only a few void defects at the sharp corner of the particles when the strain is small, and the shedding particles can hardly be observed, which is due to the large compressive stress in this direction (caused by the rolling process). With the gradual increase of strain, tearing cracks begin to appear at the hole and the edge of particles, this is because there is a large amount of stress concentration in these two places, and the stress is released with the increase of tensile stress in the process of tension. so that cracks appear here. In a word, the shedding of particles first occurs in the deformation process of SiC_p/Al composites, and then leads to the generation and propagation of matrix cracks, which are mainly caused by the void defects in the matrix itself.

In order to study the effect of tensile damage on the mechanical

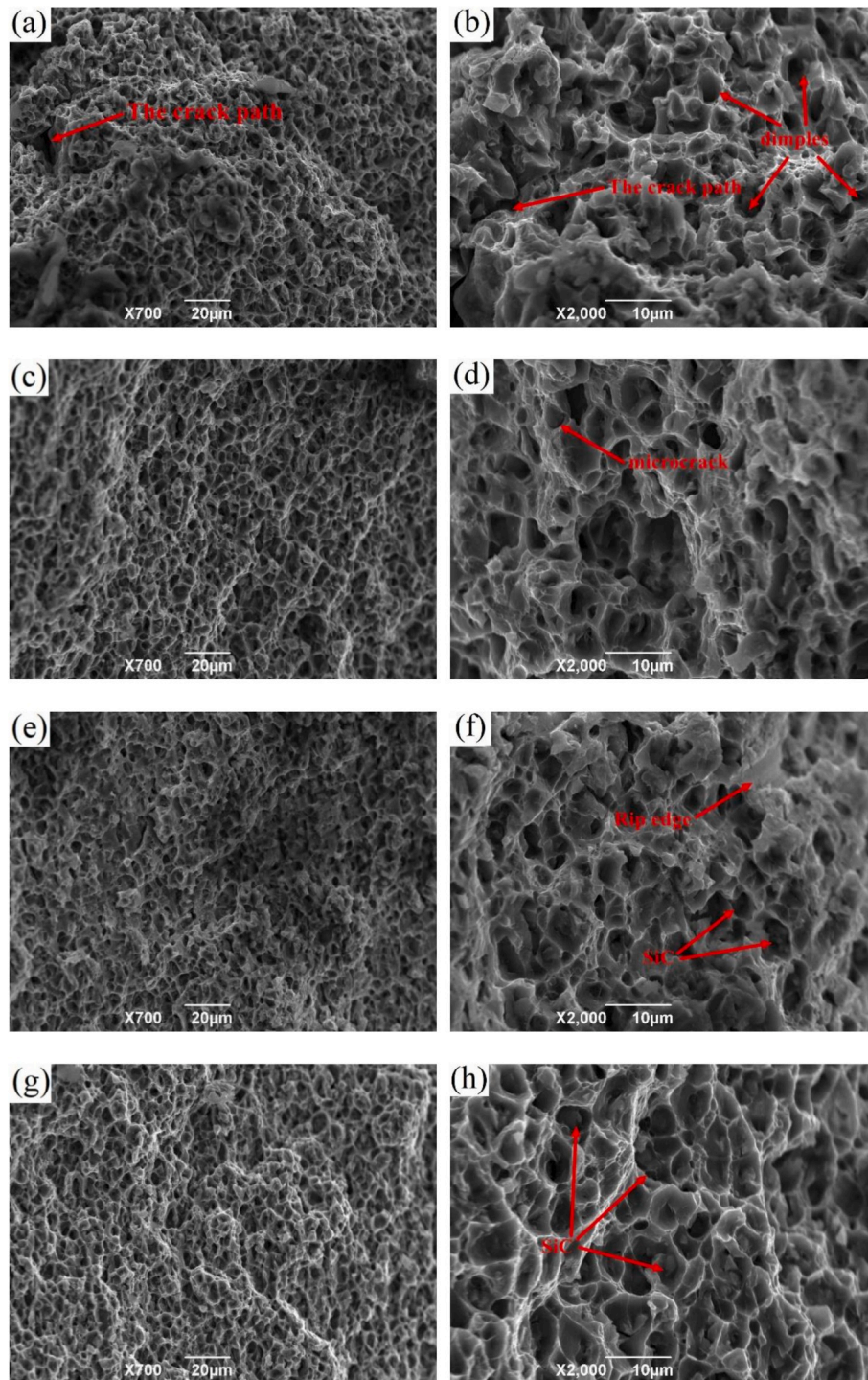


Fig. 5. Fracture scan of SiC_p/Al composite under uniaxial stretching: (a, b): 0.1 mm/min, (c, d): 0.5 mm/min, (e, f): 1 mm/min, (g, h): 2 mm/min.

properties of materials, the hardness under different strains was statistically analyzed (as shown in Fig. 7). It can be seen from the figure that in the elastic deformation stage of the composites, that is, when $\varepsilon < 0.032$, the hardness of the composites tends to decrease linearly with the increase of strain. The microhardness in three directions is $TD > RD > ND$, which is the effect of particle size [22,23]. Because the particle size in the normal direction is larger than that in other directions, its hardness is the smallest. However, the hardness value of the composite material reached the peak of the plastic deformation stage when $\varepsilon = 0.064$, and the microhardness appeared as $TD < RD < ND$ at $\varepsilon = 0.048$ and $\varepsilon = 0.064$, which is inconsistent with that the more serious the

deformation, the smaller the hardness, this should be caused by particle agglomeration. As can be seen from Fig. 6(j), (k) and (l), the original dispersed particles gradually come together with the increase of deformation. Due to the large difference in yield stress between the matrix and the particles, the matrix is more likely to deform in the process of deformation. When the deformation is serious, the particles have a small displacement relative to the matrix and gather together, so that the hardness of the composites is improved. Because the degree of deformation is different in different directions, the deformation in the rolling normal direction is more serious than that in the other two directions, and the particle concentration is more obvious, so its microhardness is

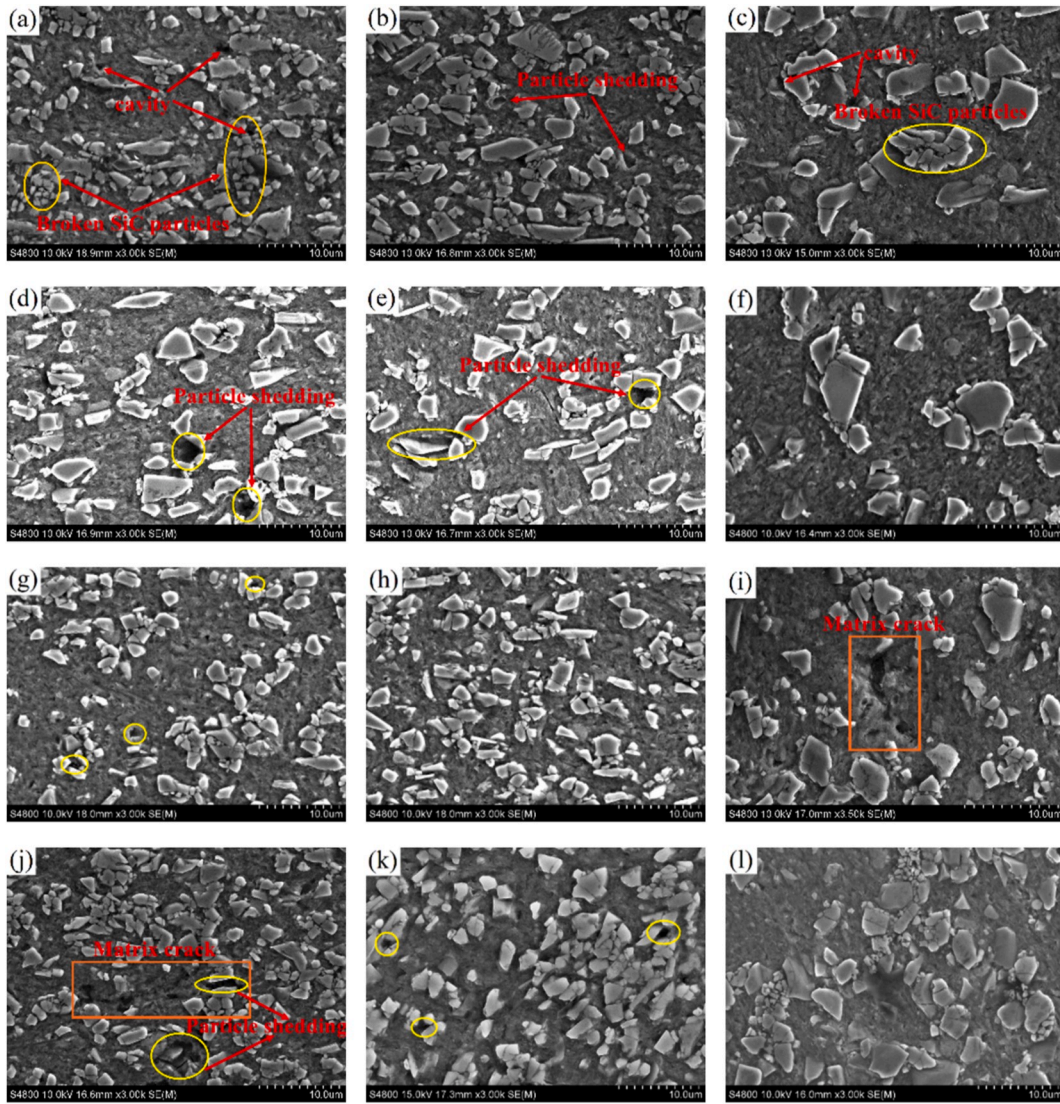


Fig. 6. SEM of composites under different tensile conditions:(a, b, c) $\epsilon = 0.016$, (d, e, f) $\epsilon = 0.032$, (g, h, i) $\epsilon = 0.048$, (j, k, l) $\epsilon = 0.064$, (a, d, g, j): RD, (b, e, h, k): TD, (c, f, i, l): ND.

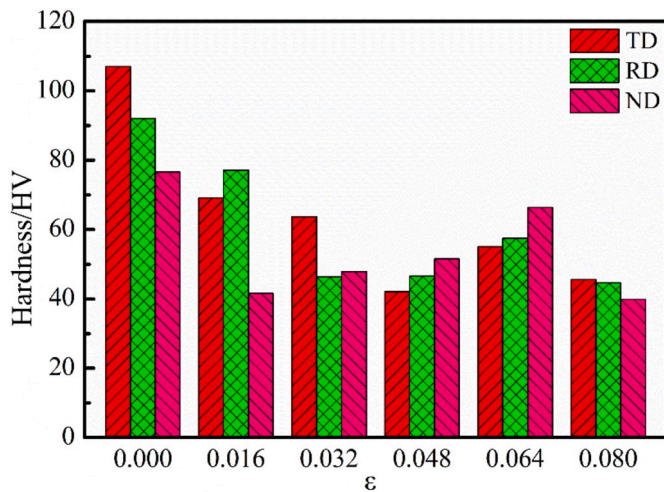


Fig. 7. Microhardness with different strains in three directions.

higher than that in the other two directions. In addition, it can be seen from Fig. 6(c), (f), (i) and (l) that some of the large fragile SiC particles break into many fine particles. With the increase of deformation, the small particles gradually distribute in the matrix, thus the number of particles increases and the particle size decreases, especially when $\epsilon = 0.064$, this phenomenon is especially obvious. So in the direction of ND, in the range of 0.016~0.064, the hardness increases with the increase of deformation strain. Therefore, during the deformation process of SiC-p/Al composites, the hardness of the composites decreased with the increase of deformation in the elastic stage, while at the plastic stage, the hardness of the composites increased due to the agglomeration of SiC particles.

The damage mechanism of the composite is the same as the “barrel principle”, which depends on the weakest microstructure. When the strength of the matrix is small, the material will crack along the matrix, and vice versa. According to the above research, the deformation law, damage behavior and fracture mechanism of the composite have been clearly understood. The damage mechanism of the composite is shown in Fig. 8. In the process of deformation and cracking of the material, the composite first produces microcracks at the holes and weak interfaces (Fig. 3(b)). With the gradual increase of deformation, small cracks converge to form large cracks (Fig. 3(c)). The shedding of particles and

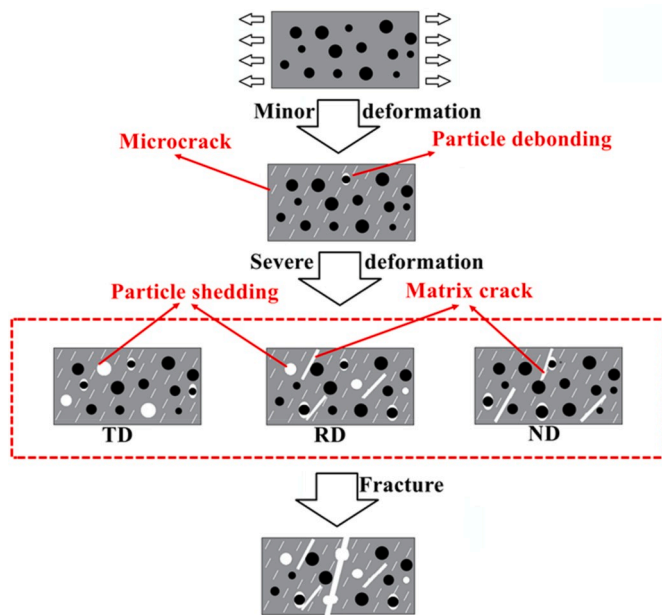


Fig. 8. Damage mechanism diagram of composites.

matrix cracks appear in the rolling direction. (Fig. 6(d) and (j)). A small amount of SiC particles also shedding in the transverse direction of rolling (Fig. 6(b) and (e)), while large matrix cracks are produced in the normal direction of rolling (Fig. 6(i)). When the resulting crack gradually spreads and widens to a certain extent (Fig. 3(f)), it begins to spread along the side (Fig. 3(d)), resulting in fracture. SiC particles (Fig. 5(f) and (h)) and matrix cracks (Fig. 5(a) and (b)) were found in the final fracture picture. It is concluded that the fracture mechanism of the composite is mainly the tearing of aluminum matrix and the shedding of

particles, there is particle debonding in the process.

3.4. Finite element analysis verification

In order to verify the damage evolution of composites during tension, a three-dimensional finite element model was constructed by using general finite element ABAQUS to simulate the tensile process. The uniaxial tensile model is shown in Fig. 9(a). The model is gridded with a three-dimensional solid element(C3D8R), and the number of meshes is 10192. The material parameters are obtained from uniaxial tensile tests as follows: density of 2.86 g/cm³, Young’s modulus of 94 GPa, and Poisson’s ratio of 0.2. In order to study the effect of particles on materials, the center of the above model with large deformation was selected for further simulation, and irregular SiC particles were randomly embedded into the Al matrix with no interface. According to the quantitative metallography theory, the volume fraction of the reinforced particles is equal to its area fraction. In the modeling process, the area of the reinforced particles is 17% of the whole model area, and the model is shown in Fig. 9(b). The three-dimensional solid element(C3D8R) is also used to griddle the particles and the matrix. Among them, the density, Young’s modulus and Poisson’s ratio of 2009Al were set to be 2.7 g/cm³, 75 GPa and 0.17. SiC particles were set to be 3.2 g/cm³, 427 GPa and 0.17, respectively. These models are subjected to uniaxial tension by defining a fixed surface on one side and a load surface on the opposite side. Except for the load surface and the fixed surface, the other surfaces are set to free boundary conditions, and the deformation conditions of the selected position in the model are given to the boundary of the sub-model. After finite element simulation, the true stress-true strain curve of the model is shown in Fig. 9(c), from which it can be seen that the curve is in good agreement with each other.

To investigate the microscopic mechanism of deformation, the stress triaxiality is adopt in this study, which describes the advantages of the void mechanism over the shear mechanism during material deformation [20]. The expression is as follows:

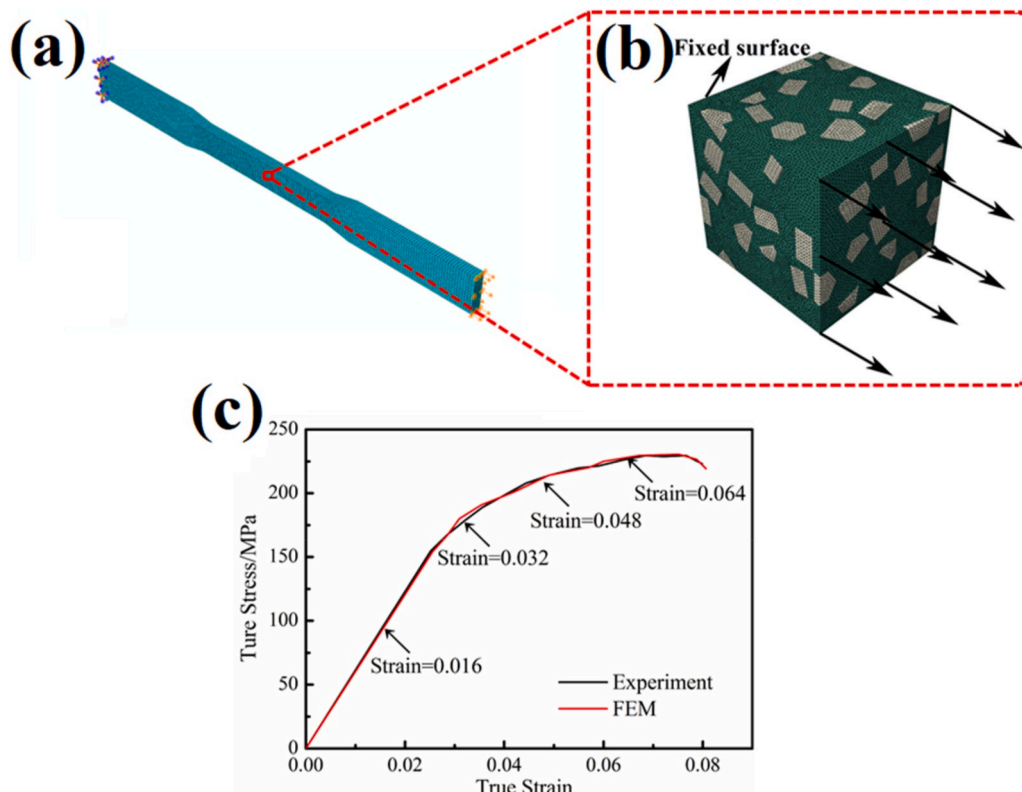


Fig. 9. Uniaxial tensile test model and true stress-true strain curve: (a) sample model, (b) local position submodel, (c) comparison of test and simulation results.

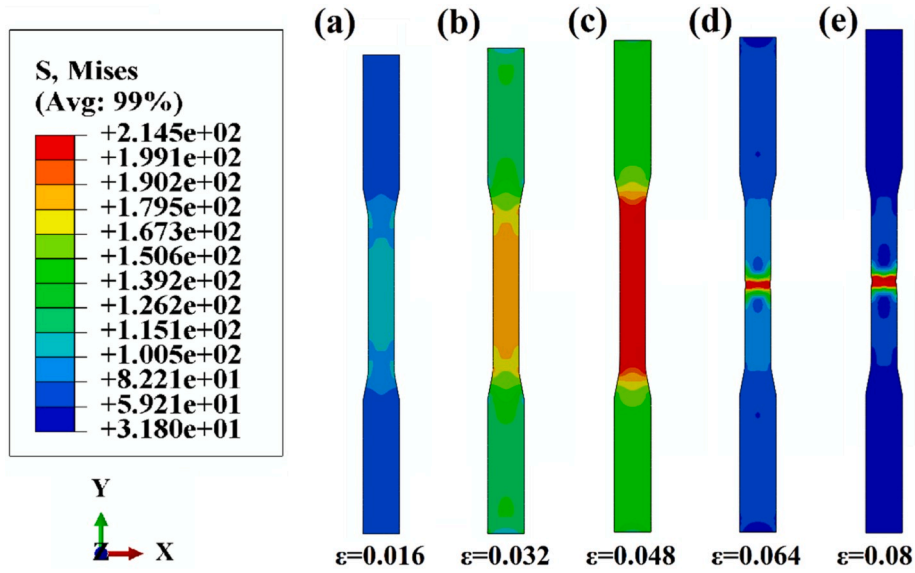


Fig. 10. Evolution of von Mises stress during tensile deformation (MPa).

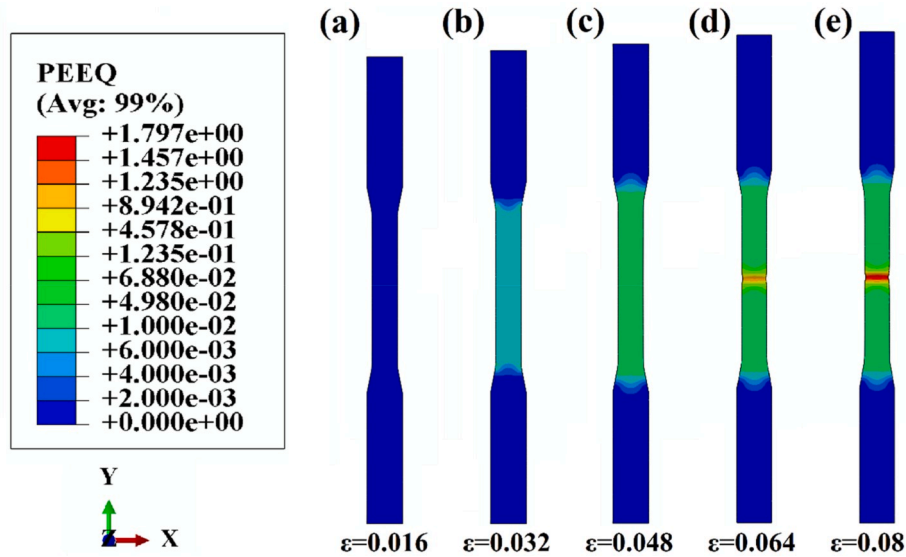


Fig. 11. Evolution of equivalent plastic strain during tensile deformation.

$$R_d = \frac{\sigma_m}{\sigma_{eq}} = \frac{(\sigma_1 + \sigma_2 + \sigma_3)/3}{\frac{1}{\sqrt{2}} \sqrt{(\sigma_1 - \sigma_2)^2 + (\sigma_2 - \sigma_3)^2 + (\sigma_3 - \sigma_1)^2}} \quad (1)$$

where σ_m and σ_{eq} are the hydrostatic stress and equivalent Von Mises stress, respectively. When the triaxial stress is high, the dimple mechanism is dominant and the hole expands rapidly. The UVARM user-subroutine for ABAQUS is adopted for the user-defined output variables of the stress triaxiality.

3.4.1. Deform parameters during the tensile test of SiC_p/Al composites

The stress evolution of SiC_p/Al composites under different strains are shown in Fig. 10, and the different stages in Fig. 10(a), (b), (c), (d) and (e) correspond to the positions indicated by the arrowheads in Fig. 9(c), respectively. As shown in the figure, the plastic deformation distribution of the material is horizontally symmetrical, Mises stress increases gradually from the loading boundary to the interior, and the maximum value is observed at the center. When $\varepsilon = 0.032$, the stress can be divided into: parallel length, transition radius, loading width and loading

boundary. The stress distribution is uniform in the range of parallel length. At the transition radius, due to the appearance of the chamfer, the shape of stress distribution is a multi-layer symmetrical ellipse, the stress value is less than the parallel length but larger than the loading width, and the upper ellipse is smaller than the lower ellipse. The stress distribution is uniform at the loading width. When $\varepsilon = 0.048$, the situation is the similar to that of $\varepsilon = 0.032$, but the stress value increases as a whole. As the strain continues to increase, the length of the model increases gradually, the stress gradually concentrates to the center and becomes more and more obvious, resulting in the final fracture of the material in the middle position.

The equivalent plastic strain of the composite with the tensile strain of 0.016, 0.032, 0.048, 0.064 and 0.08 is shown in Fig. 11. The equivalent plastic strain distribution of the composite is similar to the stress distribution, showing a symmetrical distribution and the maximum value is gradually concentrated at the center from the uniform distribution of the parallel length, and the PEEQ value increases gradually from the loading boundary to the center. When $\varepsilon = 0.016$, the material is mostly undergoing elastic deformation, plastic strain is very small. It can

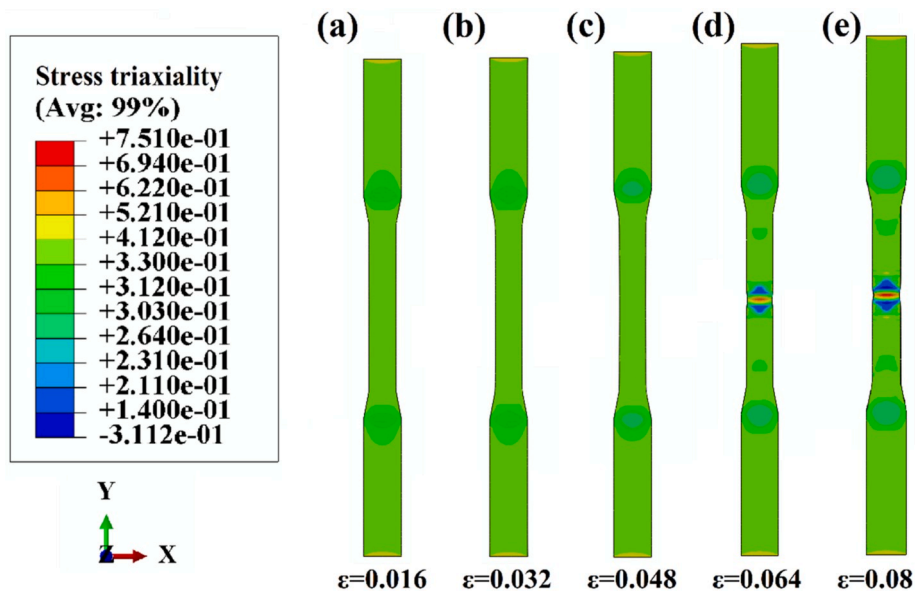


Fig. 12. Evolution of stress triaxiality during tensile deformation.

be found that the maximum peak value of $\epsilon = 0.064$ is almost 1.8. It shows that the composite material has a lot of plastic deformation at this stage. As a result, it will cause a large number of SiC particles to fall off.

The stress triaxiality of SiC_p/Al composites under different strains is shown in Fig. 12. As shown in the figure, there is no difference in the characteristics of the stress triaxiality of the first three tensile strains except for minimal changes in values. When $\epsilon = 0.064$ and $\epsilon = 0.08$, the stress triaxiality increases gradually, and the maximum stress triaxiality is seen at the center of the material. The large stress triaxiality is located in the place where the plastic deformation is small, the stress concentration is serious, the volume deformation is larger, and more elastic strain energy can be released. So the material breaks at the center. The increase of stress triaxiality not only increases the fracture tendency of the composites, but also increases the size of holes in the composites, so the formation of a large number of dimples is observed in Fig. 5. In addition, it is also found that the stress triaxiality value of the composite ranges from 0.303 to 0.412. However, under large deformation, the stress triaxiality at the center reaches 0.751, which indicates that the position is beyond the uniaxial stress state.

3.4.2. Deform parameters of SiC_p/Al composites submodel

In order to study the effect of particles on the material, the changes of stress, equivalent strain and stress triaxiality of the sub-model of the composite were studied when the strain was 0.08. The stress distribution results of the composite are shown in Fig. 13. It can be seen from Fig. 13 (a) that there is a large stress distribution on the reinforced particles,

especially at the sharp corner of the particles. The stress value is twice that of the matrix, indicating that the reinforced particles are the main stress bearing unit of the composites. The stress on the surface of the composite is much greater than that of the internal particles, and the stress on the particles decreases from the outside to the inside, and the stress on the particles also tends to decrease along the tensile direction, this is consistent with the results of J.F. Zhang et al. [24] who studied the damage and failure of SiC_p/Al composites during uniaxial tension by finite element method. It is found from the stress distribution of the composite matrix (Fig. 13(b)), the stress in the matrix around the particles is much larger than that in other positions, and there is also a large stress distribution in the interior around the particles, especially around the sharp corner particles, indicating that the reinforced particles have mutual influence on the stress distribution of the matrix materials around them. In addition, it is also found that there is more than one SiC particle around the high stress region, which indicates that the stress distribution of the composite with multiple particles affects each other. From Fig. 13(c), it can be found that there is a stress concentration region in the matrix material near the reinforced particles, a certain high stress concentration region in the matrix material between the adjacent reinforced particles, and a low stress concentration region on both sides. Due to the high stress in the deformation process between the particles and the matrix around the particles, the deformation of the particles and the matrix is not coordinated, which leads to the shedding of SiC particles.

The simulation results of the equivalent plastic strain (PEEQ)

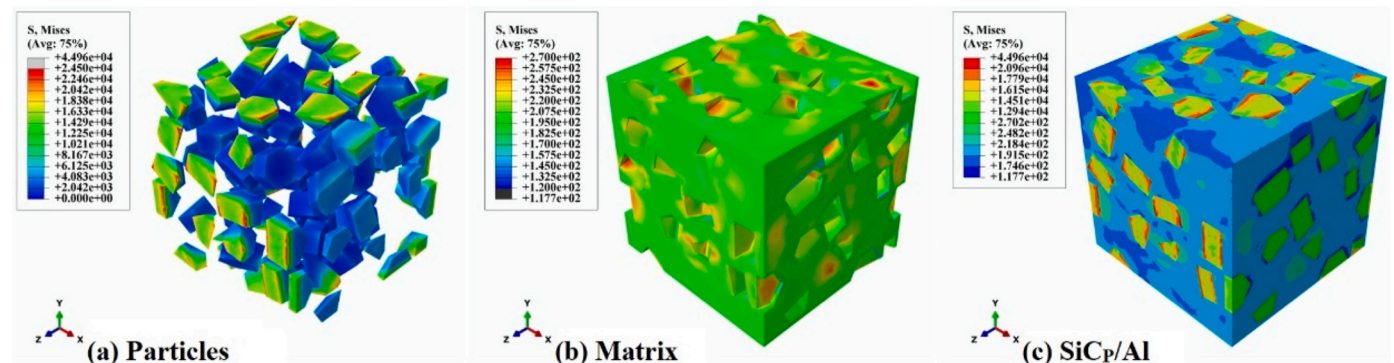


Fig. 13. Stress distribution of the composite.

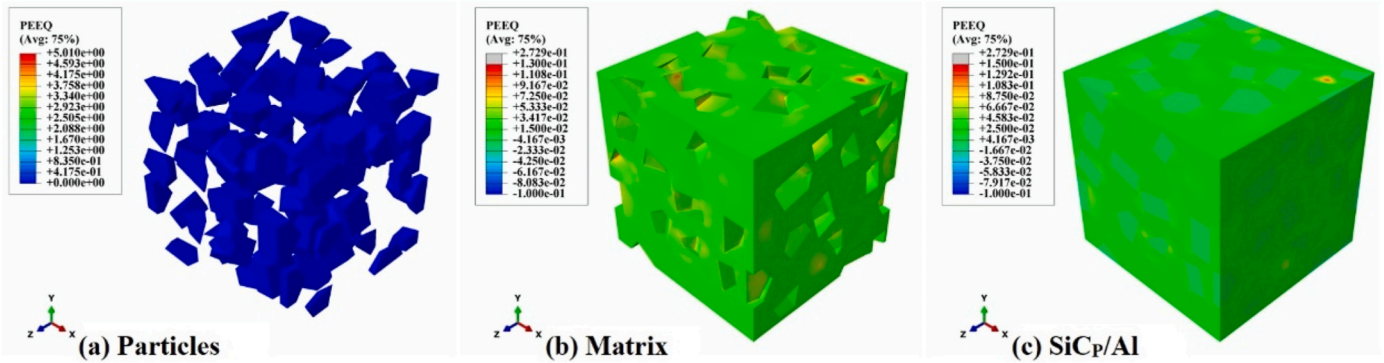


Fig. 14. Equivalent plastic strain of the composite.

distribution of the composite are shown in Fig. 14. As shown in Fig. 14 (a), the reinforced granular material is an elastomer and no plastic deformation occurs during tension. It can be seen from Fig. 14(b) that the plastic strain on the matrix is larger. The plastic strain in the region closer to the reinforced particles is larger, and the plastic strain at the position closest to the particles reaches the maximum, the maximum plastic strain of the composite material indicates that the matrix material is the main load-bearing unit for plastic strain of the composite material. There is a high plastic deformation region in the matrix material, perpendicular to the tensile direction, the interaction between the two adjacent particles results in a high plastic strain zone in its relative position, and a low plastic strain region is distributed on both sides of it. For the composite material (Fig. 14(c)), the variation range of the plastic strain of the composite is 0 to 0.13. The distribution of the maximum plastic strain of the composite is roughly similar to the stress distribution, and there is a certain interaction between the adjacent reinforced particles, resulting in a larger plastic strain between them than on both sides. There is an obvious plastic strain concentration zone on the matrix around the reinforced particles, and the plastic strain on the matrix near the particles reaches the maximum plastic deformation of the composite.

When the stress triaxiality is positive, the material tends to the tensile stress state, and the microcrack is easy to expand; when the stress triaxiality is negative, the material tends to compress the stress state and the microcrack is closed [20]. Fig. 15 shows the simulation results of stress triaxiality distribution of the composite. Fig. 15(a) and (b) are the stress triaxiality of particles and matrix materials, respectively. It can be seen from the diagram that the stress triaxiality of particles on the surface of the composite is less than 0, while that of internal particles is greater than 0, which shows that the internal particles carry tensile stress, while the surface particles carry compressive stress. On the whole, the matrix material only has the effect of tensile stress, and the stress triaxiality is larger than the particles. According to the point of view of modern damage mechanics, the fracture toughness of metals

decreases with the increase of stress triaxiality. That is, the greater the stress triaxiality in a certain range, the more brittle the material tends to be. This shows that SiC particles have a significant effect on the damage of Al alloy. In addition, it is found that the stress triaxiality of some particles at the sharp corner and near the matrix is much larger than that of others, which will cause the holes near the sharp corners to nucleate easily and gather to form cracks, resulting in the shedding of particles. This shows that the sharp corner of particles is easy to damage and crack and even cause particle fracture. Fig. 15 (c) shows the stress triaxiality of the whole material. Due to the influence of particles, the material has a large stress triaxiality and reaches the maximum value at the particle concentration, while the large stress triaxiality increases the possibility of void growth and fracture of the composite [25].

4. Conclusion

In this paper, the damage evolution of SiC_p/Al composites during tensile deformation to fracture was studied by tensile test and finite element method, and the following conclusions were drawn:

- (1) The damage process of SiC_p/Al composites includes crack initiation, crack propagation, crack connection, and the shedding of a small amount of SiC particles. With the growth and connection of microcracks and the aggregation of micropores, macroscopic cracks are formed, which finally lead to the fracture of the sample.
- (2) The fracture mechanism of SiC_p/Al composites is caused by the tearing of aluminum matrix and the shedding of particles. In the rolling transverse direction, the shedding of the particles is more serious, while in the normal direction of the rolling, the cracks in the matrix first appear, and then propagate to other directions.
- (3) According to FEM simulation results, it is found that the fracture of SiC_p/Al composites is caused by the gradual concentration of

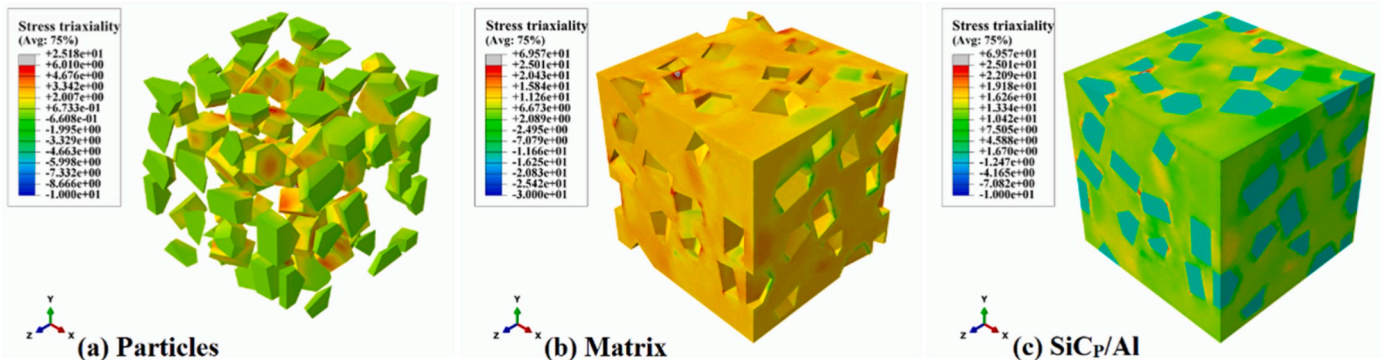


Fig. 15. Triaxiality of stress of the whole composite.

stress and strain from the whole uniform distribution to the center in the process of deformation. The increasing stress triaxiality around the particles, especially at the sharp corners, will cause the particles to fall off or debonding.

Data availability

There are no linked research data sets for this submission. The following reason is given:

Data will be made available on request.

Declaration of competing interest

We declare that we do not have any commercial or associative interest that represents a conflict of interest in connection with the work submitted.

CRediT authorship contribution statement

Qiuyan Shen: Software, Investigation, Writing - original draft. **Zhanwei Yuan:** Resources, Writing - review & editing, Supervision, Data curation. **Huan Liu:** Software, Investigation. **Xuemin Zhang:** Writing - review & editing. **Qinqin Fu:** Investigation. **Quanzhao Wang:** Investigation.

Acknowledgement

The authors are very grateful for the support received from the China Postdoctoral Science Foundation (No. 2017M623084), National Science and Technology Major Project (2017-VII-0012-0107), Fundamental Research Funds for the Central Universities, CHD (No. 310831172001, 300102319101 and 300102310201).

References

- [1] X. Guo, G. Qiang, Z. Li, G. Fan, D.B. Xiong, Y. Su, Z. Jie, C.L. Gan, Z. Di, Interfacial strength and deformation mechanism of SiC-Al composite micro-pillars, *Scripta Mater.* 114 (2016) 56–59.
- [2] S. Zou, X. Zhou, Y. Rao, X. Hua, X. Cui, Corrosion resistance of nickel-coated SiCp/Al composites in 0.05 M NaCl solution, *J. Alloys Compd.* 780 (2019) 937–947.
- [3] Q. Meng, Z. Wang, Prediction of interfacial strength and failure mechanisms in particle-reinforced metal-matrix composites based on a micromechanical model, *Eng. Fract. Mech.* 142 (2015) 170–183.
- [4] K. Jiao, S. Huang, L. Xu, D. Zhou, Feature classification of high-volume SiCp/Al composites under the condition of two-dimensional cutting based on cluster analysis theory, *Int. J. Adv. Manuf. Technol.* 78 (5–8) (2014) 677–686.
- [5] P. Hruby, S.S. Singh, J.J. Williams, X.H. Xiao, F. De Carlo, N. Chawla, Fatigue crack growth in SiC particle reinforced Al alloy matrix composites at high and low R-ratios by in situ X-ray synchrotron tomography, *Int. J. Fatig.* 68 (2014) 136–143.
- [6] L. Zhou, S. Huang, L. Xu, D. Bai, P. Zhao, Drilling characteristics of SiCp/Al composites with electroplated diamond drills, *Int. J. Adv. Manuf. Technol.* 69 (5–8) (2013) 1165–1173.
- [7] K.K. Chawla, N. Chawla, *Metal Matrix Composites: Automotive Applications*, 2014.
- [8] J.J. Williams, Z. Flom, A.A. Amell, N. Chawla, X. Xiao, F. De Carlo, Damage evolution in SiC particle reinforced Al alloy matrix composites by X-ray synchrotron tomography, *Acta Mater.* 58 (18) (2010) 6194–6205.
- [9] M. Schobel, W. Altendorfer, H.P. Degischer, S. Vaucher, T. Buslaps, M. Di Michiel, M. Hofmann, Internal stresses and voids in SiC particle reinforced aluminum composites for heat sink applications, *Compos. Sci. Technol.* 71 (5) (2011) 724–733.
- [10] I.A. Ibrahim, F.A. Mohamed, E.J. Lavernia, Particulate reinforced metal matrix composites-a review, *J. Mater. Sci. (USA)* 26 (5) (1991) 1137–1156.
- [11] H. Qing, 2D micromechanical analysis of SiC/Al metal matrix composites under tensile, shear and combined tensile/shear loads, *Mater. Des.* 51 (2013) 438–447.
- [12] H. Qing, T.L. Liu, Micromechanical analysis of SiC/Al metal matrix composites: finite element modeling and damage simulation, *Int. J. App. Mech.* 7 (2) (2015).
- [13] A. Paknia, A. Pramanik, A.R. Dixit, S. Chattopadhyaya, Effect of size, content and shape of reinforcements on the behavior of metal matrix composites (MMCs) under tension, *J. Mater. Eng. Perform.* 25 (10) (2016) 4444–4459.
- [14] J.J. Williams, J. Segurado, J. Llorca, N. Chawla, Three dimensional (3D) microstructure-based modeling of interfacial decohesion in particle reinforced metal matrix composites, *Mater. Sci. Eng., A* 557 (1) (2012) 113–118.
- [15] J.F. Zhang, H. Andr , X.X. Zhang, Q.Z. Wang, B.L. Xiao, Z.Y. Ma, An enhanced finite element model considering multi strengthening and damage mechanisms in particle reinforced metal matrix composites, *Compos. Struct.* 226 (2019), 111281.
- [16] G.G. Sozhamannan, S.B. Prabu, R. Paskaramoorthy, Failures analysis of particle reinforced metal matrix composites by microstructure based models, *Mater. Des.* 31 (8) (2010) 3785–3790.
- [17] Z. Jie, Q. Ouyang, G. Qiang, Z. Li, G. Fan, Y. Su, J. Lin, E.J. Lavernia, J. M. Schoenung, Z. Di, 3D Microstructure-based finite element modeling of deformation and fracture of SiCp/Al composites, *Compos. Sci. Technol.* 123 (2016) 1–9.
- [18] R. Ekici, M. Kemal Apalak, M. Yildirim, F. Nair, Effects of random particle dispersion and size on the indentation behavior of SiC particle reinforced metal matrix composites, *Mater. Des.* 31 (6) (2010) 2818–2833.
- [19] S. Niemsakul, N. Sae-Eawa, Y. Aue-U-Lan, Determination and analysis of critical damage criteria for predicting fracture in forming process by uniaxial tensile test, *Mater. Today: Proc.* 5 (3) (2018) 9642–9650.
- [20] Z. Yuan, F. Li, F. Xue, M. He, M.Z. Hussain, Analysis of the stress states and interface damage in a particle reinforced composite based on a micromodel using cohesive elements, *Mater. Sci. Eng. A* 589 (2014) 288–302.
- [21] J.F. Zhang, X.X. Zhang, Q.Z. Wang, B.L. Xiao, Z.Y. Ma, Simulation of anisotropic load transfer and stress distribution in sicp/Al composites subjected to tensile loading, *Mech. Mater.* 122 (2018) 96–103.
- [22] Z.W. Wang, M. Song, C. Sun, Y.H. He, Effects of particle size and distribution on the mechanical properties of SiC reinforced Al-Cu alloy composites, *Mater. Sci. Eng. Struct. Mater. Prop. Microstruct. Proc.* 528 (3) (2011) 1131–1137.
- [23] Y.W. Yan, L. Geng, Effects of particle size on deformation behaviour of metal matrix composites, *Mater. Sci. Technol.* 23 (3) (2013) 374–378.
- [24] J.F. Zhang, X.X. Zhang, Q.Z. Wang, B.L. Xiao, Z.Y. Ma, Simulations of deformation and damage processes of SiCp/Al composites during tension, *J. Mater. Sci. Technol.* 34 (4) (2018) 627–634.
- [25] V.V. Ganesh, N. Chawla, Effect of particle orientation anisotropy on the tensile behavior of metal matrix composites: experiments and microstructure-based simulation, *Mater. Sci. Eng. A* 391 (1–2) (2005) 342–353.